Pramana – J. Phys. (2017) 89:23
DOI 10.1007/s12043-017-1418-8

New interior solution describing relativistic fluid sphere

KSH NEWTON SINGH[1,*], NARENDRA PRADHAN[1] and NEERAJ PANT[2]

[1]Department of Physics, National Defence Academy, Khadakwasla, Pune 411 023, India
[2]Department of Mathematics, National Defence Academy, Khadakwasla, Pune 411 023, India
*Corresponding author. E-mail: ntnphy@gmail.com

MS received 8 August 2016; revised 21 December 2016; accepted 25 January 2017; published online 11 July 2017

Abstract. A new exact solution of embedding class I is presented for a relativistic anisotropic massive fluid sphere. The new exact solution satisfies Karmarkar condition, is well-behaved in all respects, and therefore is suitable for the modelling of superdense stars. Consequently, using this solution, we have studied in detail two compact stars, namely, XTE J1739-289 (strange star $1.51M_\odot$, 10.9 km) and PSR J1614-2230 (neutron star $1.97M_\odot$, 14 km). The solution also satisfies all energy conditions with the compactness parameter lying within the Buchdahl limit.

Keywords. General relativity; exact solution; embedding class I; anisotropy; compact star.

PACS Nos **02.60.Cb; 04.20.–q; 04.20.Jb; 04.40.Nr; 04.40.Dg**

1. Introduction

Any four-dimensional flat space can be considered embedded in higher-dimensional pseudo-Euclidean space (Eddington [1]). Any manifold V_n can be embedded in $m = (n(n+1)/2)$-dimensional pseudo-Euclidean space E_m. The minimum extra dimension p to embed the manifold V_n into E_m is the class of the manifold V_n and is $\leq m - n = n(n-1)/2$. Therefore, the class of relativistic space–time manifold V_4 is VI. All the spherically symmetric space–times are in general of class II and plane symmetric space–times are of class III. However, the entire spherically symmetric manifold is of class I if it satisfies Karmarkar condition [2] along with $R_{2323} \neq 0$ [3]. In fact, the well-known Friedman–Robertson–Lemaitre [4] cosmological solution is of class I. Indeed, the first exact Schwarzschild exterior solution is of class II and Schwarzschild interior solution [5] is of class I. The most realistic exterior solution describing a spinning black hole, the Kerr metric, is of class V [6]. Embedding class of space took vital role in describing the internal symmetry of elementary particle physics [7]. Pavsic and Tapia [8] have discussed the applications of embedding solution to general relativity, extrinsic gravity, strings and new brane world. For any neutral and isotropic fluid distributions, the solutions of Einstein field equations (EFEs) that do satisfy Karmarkar condition is either Schwarzschild interior [5] or Kohlar–Chao [9] solution. However, if we incorporate the anisotropy or electric charge or both, we may generate many new class-I solutions. Recently, many researchers have published some well-behaved class-I solutions of Einstein field equations [10–16]. All these solutions are compatible for modelling massive relativistic superdense stars.

In the present article, we adopted the Karmarkar condition to generate a completely new class-I solution with ansatz g_{rr} on account of anisotropy. The article is organized as follows: Section 3 is devoted to EFEs and Karmarkar condition and in §4 we adopted an algorithm to generate a new anisotropic class-I solution. In §5 we have discussed the properties of the new solution and its behaviour at the centre of the fluid sphere. The matching of interior and exterior space–time at the boundary is discussed in §6 and in §7 we have presented the overall picture and final discussion of the solution.

2. Conditions for well-behaved solutions

Well-behaved solutions of anisotropic fluid sphere should satisfy the following conditions:

(1) The solution should be free from physical and geometric singularities, i.e. it should yield finite and positive values of the central pressure, central density and nonzero positive value of $(e^{\nu})_{r=0}$ and $(e^{\lambda})_{r=0} = 1$.

(2) The causality condition should be obeyed, i.e. velocity of sound should be less than that of light throughout the model. In addition, the velocity of sound should be decreasing towards the surface, i.e.,

$$\frac{\mathrm{d}}{\mathrm{d}r}\frac{\mathrm{d}p_r}{\mathrm{d}\rho} < 0 \quad \text{or} \quad \frac{\mathrm{d}^2 p_r}{\mathrm{d}\rho^2} > 0$$

and

$$\frac{\mathrm{d}}{\mathrm{d}r}\frac{\mathrm{d}p_t}{\mathrm{d}\rho} < 0 \quad \text{or} \quad \frac{\mathrm{d}^2 p_t}{\mathrm{d}\rho^2} > 0$$

for $0 \le r \le r_b$, i.e. the velocity of sound is increasing with the increase of density and it should be decreasing outward.

(3) The adiabatic index, $\Gamma = \frac{\rho+p_r}{p_r}\frac{\mathrm{d}p_r}{\mathrm{d}\rho}$ for the realistic matter should be $\ge 4/3$.

(4) The red shift z should be positive, finite and monotonically decreasing in nature with the increase of r.

(5) The anisotropy factor Δ should be zero at the centre and increasing towards the surface.

(6) For a stable anisotropic compact star, $-1 < v_t^2 - v_r^2 < 0$ must be satisfied (Herrera and Santos [17]).

3. Einstein–Maxwell field equations of anisotropic fluid distribution

The interior metric of a static spherically symmetric matter distribution in curvature coordinates is given by

$$\mathrm{d}s^2 = -\mathrm{e}^{\nu(r)}\mathrm{d}t^2 + \mathrm{e}^{\lambda(r)}\mathrm{d}r^2 + r^2(\mathrm{d}\theta^2 + \sin^2\theta\,\mathrm{d}\phi^2). \quad (1)$$

For our model the energy–momentum tensor for the stellar fluid is given by

$$T_{ab} = \mathrm{diag}(\rho, -p_r, -p_t, -p_t), \quad (2)$$

where ρ, p_r and p_t are the energy density, radial pressure and tangential pressure respectively.

The Einstein field equations for the line element (1) are

$$8\pi\rho(r) = \frac{\lambda'}{r}\mathrm{e}^{-\lambda} + \frac{1-\mathrm{e}^{-\lambda}}{r^2} \quad (3)$$

$$8\pi p_r(r) = \frac{\nu'}{r}\mathrm{e}^{-\lambda} - \frac{1-\mathrm{e}^{-\lambda}}{r^2} \quad (4)$$

$$8\pi p_t(r) = \mathrm{e}^{-\lambda}\left(\frac{\nu''}{2} - \frac{\lambda'\nu'}{4} + \frac{\nu'^2}{4} + \frac{\nu'-\lambda'}{2r}\right), \quad (5)$$

where prime (′) denotes the differentiation with respect to r.

In generating the above field equations we have used geometrized units where the coupling constant and the speed of light are taken to be unity. Using eqs (4) and (5) we get

$$\Delta(r) = 8\pi(p_t - p_r) = \mathrm{e}^{-\lambda}\left(\frac{\nu''}{2} - \frac{\lambda'\nu'}{4} + \frac{\nu'^2}{4} - \frac{\nu'+\lambda'}{2r} + \frac{\mathrm{e}^{\lambda}-1}{r^2}\right), \quad (6)$$

where $\Delta = 8\pi(p_t - p_r)$ is the measure of anisotropy.

If metric (1) satisfies the Karmarkar condition [2], it can represent an embedding class-I space-time, i.e.

$$R_{1414} = \frac{R_{1212}R_{3434} + R_{1224}R_{1334}}{R_{2323}} \quad (7)$$

with $R_{2323} \neq 0$ [3]. This condition leads to a differential equation given by

$$\frac{2\nu''}{\nu'} + \nu' = \frac{\lambda'\mathrm{e}^{\lambda}}{\mathrm{e}^{\lambda}-1}. \quad (8)$$

On integration we get the relationship between ν and λ as

$$\mathrm{e}^{\nu} = \left(A + B\int\sqrt{\mathrm{e}^{\lambda}-1}\,\mathrm{d}r\right)^2, \quad (9)$$

where A and B are constants of integration.

By using (9) we can rewrite (6) as

$$\Delta(r) = \frac{\nu'}{4\mathrm{e}^{\lambda}}\left[\frac{2}{r} - \frac{\lambda'}{\mathrm{e}^{\lambda}-1}\right]\left[\frac{\nu'\mathrm{e}^{\nu}}{2rB^2} - 1\right]. \quad (10)$$

4. A new class of well-behaved embedding class-I solution

To solve eq. (9), we have assumed a new g_{rr} metric potential given by

$$\mathrm{e}^{\lambda} = 1 + ar^2(1+br^2)^3, \quad (11)$$

where a and b are non-zero constants. Substituting eq. (11) in eq. (9) we get

$$\mathrm{e}^{\nu} = \left[A + \frac{B\sqrt{a}}{5b}(1+br^2)^{5/2}\right]^2, \quad (12)$$

where A and B are arbitrary constants.

On using (11) and (12) we get the expressions for density, pressures and anisotropy as

$$8\pi\rho(r) = \frac{a(1+br^2)^2[3+9br^2+ar^2(1+br^2)^4]}{[1+ar^2(1+br^2)^3]^2} \tag{13}$$

$$8\pi p_r(r) = \frac{\sqrt{a(1+br^2)^3}[5b(2B - A\sqrt{a(1+br^2)^3}) - aB(1+br^2)^4]}{[1+ar^2(1+br^2)^3][5Ab + B(1+br^2)\sqrt{a(1+br^2)^3}]} \tag{14}$$

$$\Delta(r) = \frac{r^2[a(1+br^2)^4 - 3b]}{(1+br^2)[1+ar^2(1+br^2)^3]^2[5Ab + B(1+br^2)\sqrt{a(1+br^2)^3}]}$$
$$\times [-5bB\sqrt{a(1+br^2)^3} + a(1+br^2)^3\{5Ab + B(1+br^2)\sqrt{a(1+br^2)^3}\}] \tag{15}$$

$$8\pi p_t(r) = \frac{[5Ab + B(1+br^2)\sqrt{a(1+br^2)^3}\,]^{-1}}{(1+br^2)[1+ar^2(1+br^2)^3]^2}[5bB\sqrt{a(1+br^2)^3}(2+5br^2)$$
$$-a(1+br^2)^3\{5Ab(1+4br^2) + B\sqrt{a(1+br^2)^3}(1-b^2r^4)\}]. \tag{16}$$

Now the density and pressure gradients can be written as

$$8\pi\frac{\mathrm{d}\rho}{\mathrm{d}r} = -\frac{2ar(1+br^2)}{[1+ar^2(1+br^2)^3]^3}\{a^2r^2(1+br^2)^8 - 3b(5+9br^2) + a(1+br^2)^3(5+19br^2+38b^2r^4)\} \tag{17}$$

$$8\pi\frac{\mathrm{d}p_r}{\mathrm{d}r} = -\frac{2\sqrt{a(1+br^2)^3}\{5b^2f_2(r) + ab(1+br^2)^3f_3(r) - f_1(r)\}}{(1+br^2)[1+ar^2(1+br^2)^3]^2\{5Ab + B(1+br^2)\sqrt{a(1+br^2)^3}\}^2} \tag{18}$$

$$8\pi\frac{\mathrm{d}p_t}{\mathrm{d}r} = -\frac{\sqrt{a(1+br^2)^3}\{5b^2f_4(r) - a^2B(1+br^2)^7f_5(r) + ab(1+br^2)^3f_6(r)\}}{(1+br^2)^2\{1+ar^2(1+br^2)^3\}^3\{5Ab + B(1+br^2)\sqrt{a(1+br^2)^3}\}^2} \tag{19}$$

$$f_1(r) = a^2B(1+br^2)^8\{10Abr + B(1+br^2)\sqrt{ar^2(1+br^2)^3}\}$$

$$f_2(r) = -15AbBr + 15A^2b\sqrt{ar^2(1+br^2)^3} + 2B^2(1+br^2)\sqrt{ar^2(1+br^2)^3}$$

$$f_3(r) = -25A^2b(1+br^2)\sqrt{ar^2(1+br^2)^3} + 5AbBr(16+31br^2) + B^2\sqrt{ar^2(1+br^2)^3} \times (13+66br^2+53b^2r^4)$$

$$f_4(r) = 60A^2b\sqrt{ar^2(1+br^2)^3}(1+2br^2) - 15AbBr(4+5br^2) + 2B^2\sqrt{ar^2(1+br^2)^3} \times (4br^2+5b^2r^4-1)$$

$$f_5(r) = 5Abr(8+30br^2+55b^2r^4) - 2B\sqrt{ar^2(1+br^2)^3}(5b^3r^6 - 7br^2 - 2)$$

$$f_6(r) = -100A^2b\sqrt{ar^2(1+br^2)^3} \times (1+5br^2+10b^2r^4) + 15AbBr(18+69br^2+106b^2r^4) + 6B^2\sqrt{ar^2(1+br^2)^3} \times (7+48br^2+115b^2r^4+74b^3r^6).$$

5. Properties of the new solution

The central values of pressures and density are given by

$$[8\pi p_r]_{r=0} = [8\pi p_t]_{r=0} \times \frac{10bB\sqrt{a} - aB\sqrt{a} - 5Aab}{5Ab + B\sqrt{a}} > 0 \tag{20}$$

$$[8\pi\rho]_{r=0} = 3a > 0, \quad \forall a > 0. \tag{21}$$

The Zeldovich's condition can be written as

$$\left[\frac{p_r}{\rho}\right]_{r=0} = \frac{10bB\sqrt{a} - aB\sqrt{a} - 5Aab}{3a(5Ab + B\sqrt{a})} \leq 1. \quad (22)$$

The constraint on values of A and B can be determined from eqs (20) and (22)

$$\frac{5b\sqrt{a}}{10b - a} \leq \frac{B}{A} \leq \frac{10b\sqrt{a}}{5b - 2a}. \quad (23)$$

Now the speed of sound in the stellar interior can be determined by using

$$v_r^2 = \frac{\mathrm{d}p_r/\mathrm{d}r}{\mathrm{d}\rho/\mathrm{d}r} \quad \text{and} \quad v_t^2 = \frac{\mathrm{d}p_t/\mathrm{d}r}{\mathrm{d}\rho/\mathrm{d}r}. \quad (24)$$

For a stable anisotropic model, $-1 < v_t^2 - v_r^2 < 0$ needs to be satisfied.

The relativistic adiabatic index (Γ) is given by

$$\Gamma(r) = \frac{\rho + p_r}{p_r}\frac{\mathrm{d}p}{\mathrm{d}\rho}. \quad (25)$$

For a realistic matter, it should be more than 4/3 for a stable configuration [18].

The Tolman–Oppenheimer–Volkoff (TOV) equation for the anisotropic fluid distribution can be written as

$$-\frac{M_g(\rho + p_r)}{r^2}\mathrm{e}^{(\lambda-\nu)/2} - \frac{\mathrm{d}p_r}{\mathrm{d}r} + \frac{2\Delta}{r} = 0, \quad (26)$$

where

$$M_g(r) = \frac{r^2\nu'}{2}\mathrm{e}^{(\nu-\lambda)/2}. \quad (27)$$

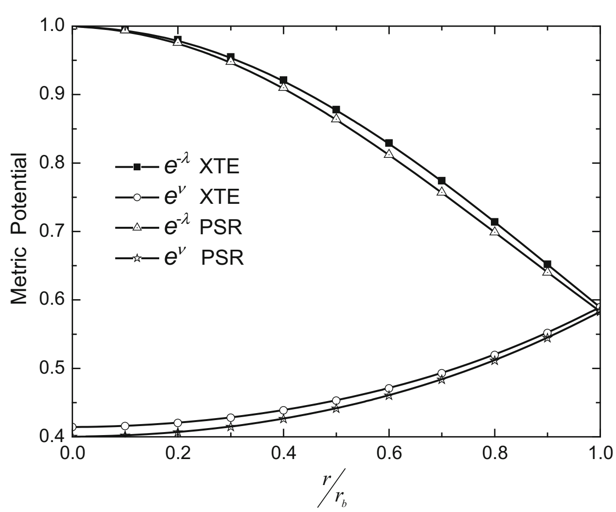

Figure 1. Variation of metric potentials with radius for XTE J1739-289 and PSR J1614-2230 for the parameters given in table 1.

Equation (26) can be written in terms of the balanced force equation due to anisotropy (F_a), gravity (F_g) and hydrostatic (F_h), i.e.

$$F_g + F_h + F_a = 0. \quad (28)$$

Here

$$F_g = -\frac{\rho + p_r}{2}\nu' \quad (29)$$

$$F_h = -\frac{\mathrm{d}p_r}{\mathrm{d}r} \quad (30)$$

$$F_a = \frac{2\Delta}{r}. \quad (31)$$

6. Boundary conditions

The interior solution so obtained are matched with the exterior solution of Schwarszchild given by

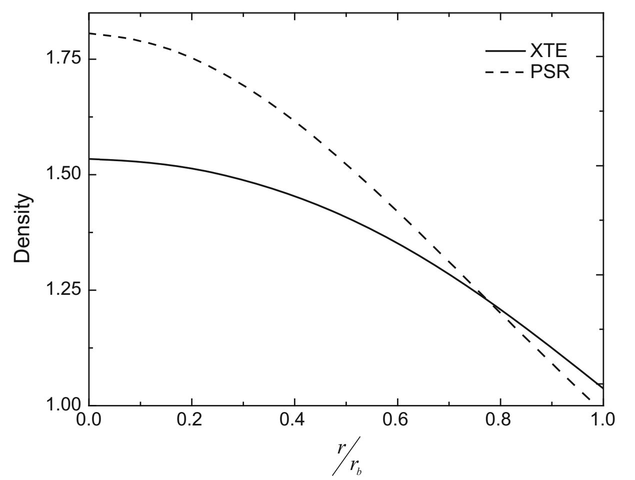

Figure 2. Variation of density with radius for XTE J1739-289 and PSR J1614-2230 for the parameters given in table 1.

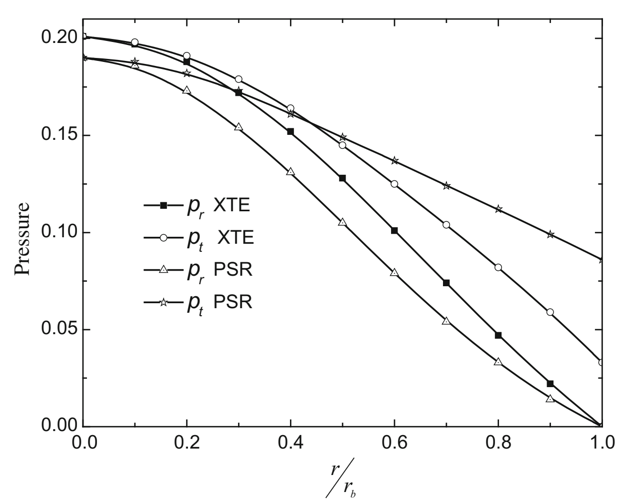

Figure 3. Variation of pressure with radius for XTE J1739-289 and PSR J1614-2230 for the parameters given in table 1.

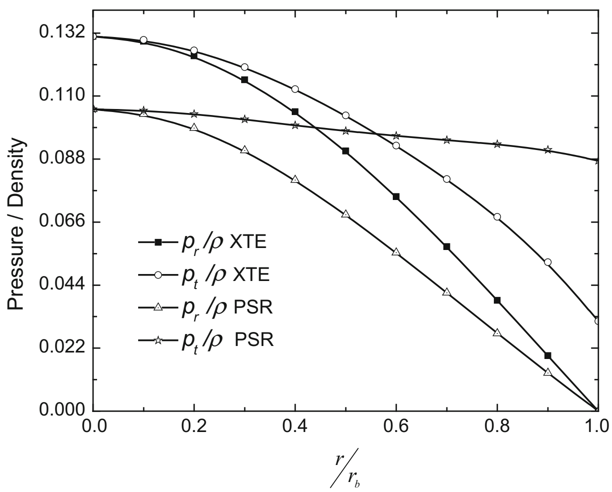

Figure 4. Variation of pressure to density ratio with radius for XTE J1739-289 and PSR J1614-2230 for the parameters given in table 1.

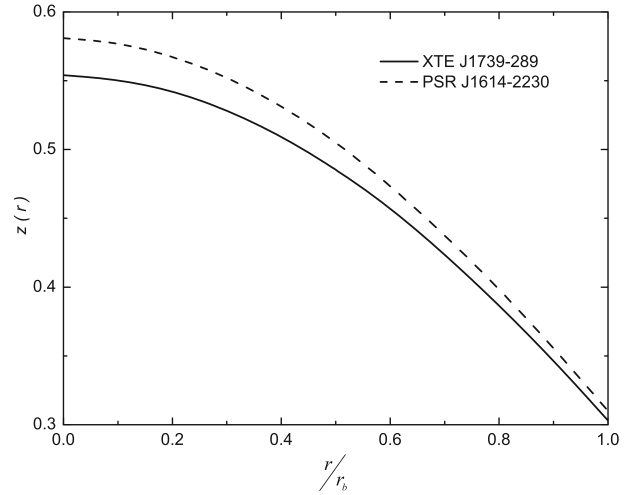

Figure 6. Variation of red-shift with radius for XTE J1739-289 and PSR J1614-2230 for the parameters given in table 1.

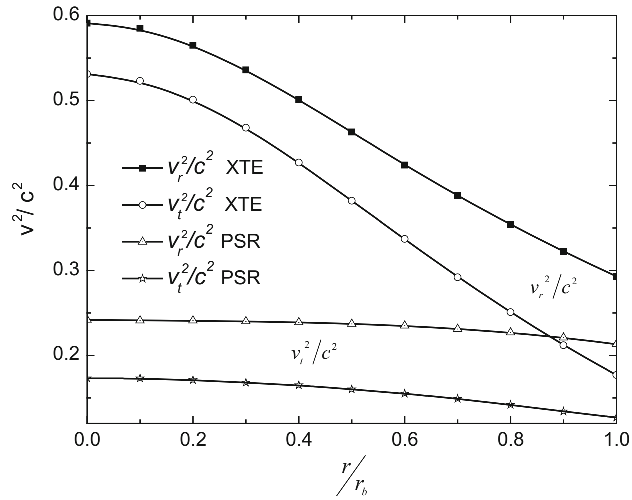

Figure 5. Variation of sound speed square with radius for XTE J1739-289 and PSR J1614-2230 for the parameters given in table 1.

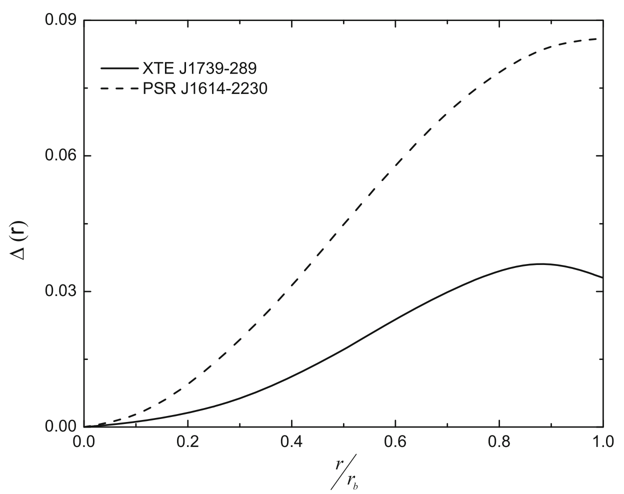

Figure 7. Variation of anisotropy with radius for XTE J1739-289 and PSR J1614-2230 for the parameters given in table 1.

$$ds^2 = -\left(1 - \frac{2M}{r}\right)dt^2 + \left(1 - \frac{2M}{r}\right)^{-1} dr^2 + r^2(d\theta^2 + \sin^2\theta d\phi^2), \tag{32}$$

where M the mass of the fluid ball as determined by an external observer at $r \geq R$ is the radial coordinate of the exterior region. We shall arrive at the following conclusions by matching exterior solution (32) with our interior solution (1) at the boundary $r = R$:

$$e^{\nu_b} = \left(1 - \frac{2M}{R}\right) = \left[A + \frac{B\sqrt{a}}{5b}(1 + bR^2)^{5/2}\right]^2 \tag{33}$$

$$e^{-\lambda_b} = (1 - \frac{2M}{R}) = \frac{1}{1 + aR^2(1 + bR^2)^3} \tag{34}$$

$$p_r(r = R) = 0. \tag{35}$$

Using boundary conditions (33)–(35), we can determine the constants as

$$A = \frac{1}{\sqrt{1 + aR^2(1 + bR^2)^3}} \left[1 + \frac{a(1+bR^2)^4}{b\left[10 - aR^2(1+bR^2)^3\right] - a(1+bR^2)^3}\right]^{-1} \tag{36}$$

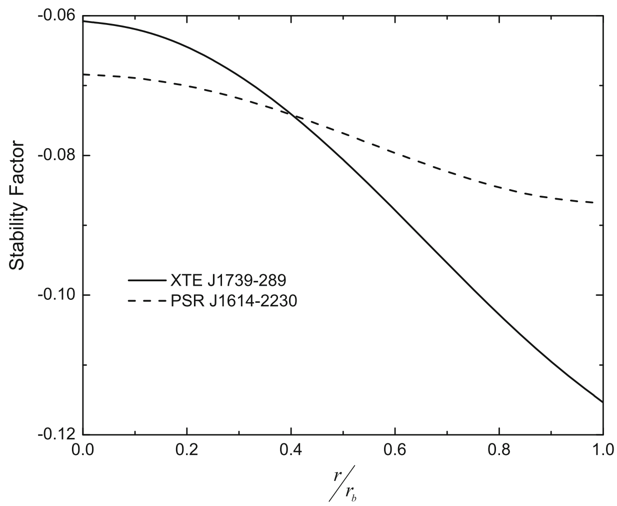

Figure 8. Variation of stability factor with radius for XTE J1739-289 and PSR J1614-2230 for the parameters given in table 1.

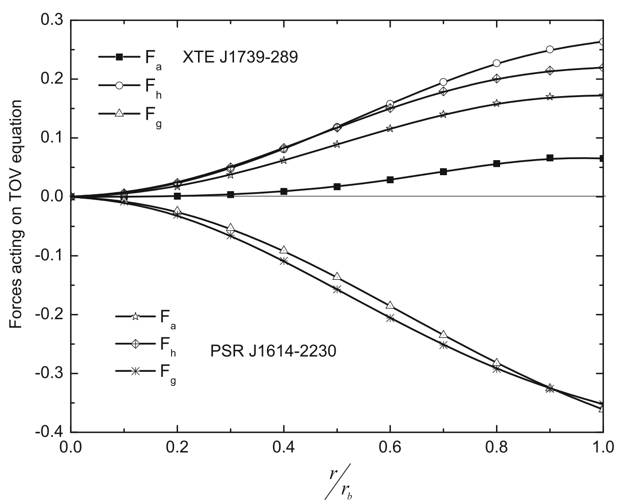

Figure 9. Variation of three different forces acting on TOV-equation with radius for XTE J1739-289 and PSR J1614-2230 for the parameters given in table 1.

$$B = \frac{5Ab\sqrt{a}\,(1+bR^2)^{3/2}}{b[10 - aR^2(1+bR^2)^3] - a(1+bR^2)^3} \tag{37}$$

$$a = \frac{1}{R^2(1+bR^2)^3}\left[\frac{1}{1-2M/R} - 1\right] \tag{38}$$

$$\frac{2M}{R} = 1 - \frac{1}{1+aR^2(1+bR^2)^3}. \tag{39}$$

Now the gravitational red-shift at the surface and within the interior of the stellar system are given respectively by

$$z_s = \mathrm{e}^{-\nu_b/2} - 1 = \left[A + \frac{B\sqrt{a}}{5b}\left(1+bR^2\right)^{5/2}\right]^{-1} - 1 \tag{40}$$

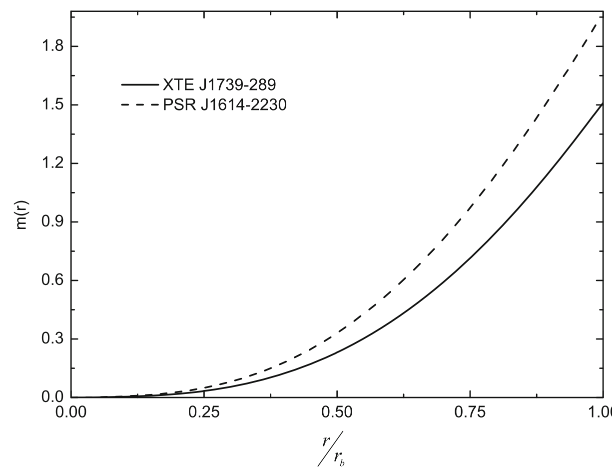

Figure 10. Variation of mass with radius for XTE J1739-289 and PSR J1614-2230 for the parameters given in table 1.

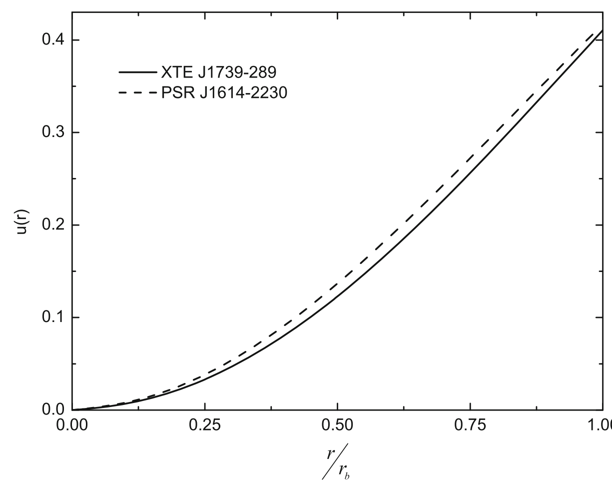

Figure 11. Variation of compactness parameter with radius for XTE J1739-289 and PSR J1614-2230 for the parameters given in table 1.

$$z(r) = \left[A + \frac{B\sqrt{a}}{5b}(1+br^2)^{5/2}\right]^{-1} - 1. \tag{41}$$

The mass function and the compactness parameter are given as

$$m(r) = 4\pi\int_0^r \rho(r) r^2 \mathrm{d}r = \frac{ar^3(1+br^2)^3}{2+2ar^2(1+br^2)^3}$$

$$u(r) = \frac{2m(r)}{r} = \frac{ar^2(1+br^2)^3}{1+ar^2(1+br^2)^3}. \tag{42}$$

Our presented solutions satisfy all the energy conditions, such as null energy condition (NEC), weak energy condition (WEC), strong energy condition (SEC) and dominant energy condition (DEC) throughout the interior region:

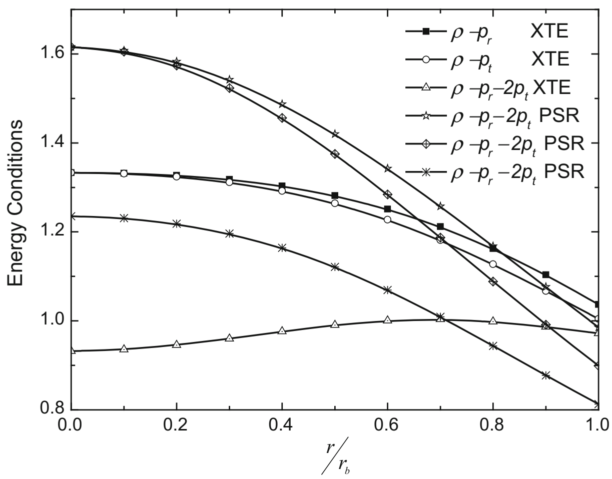

Figure 12. Variation of energy conditions with radius for XTE J1739-289 and PSR J1614-2230 for the parameters given in table 1.

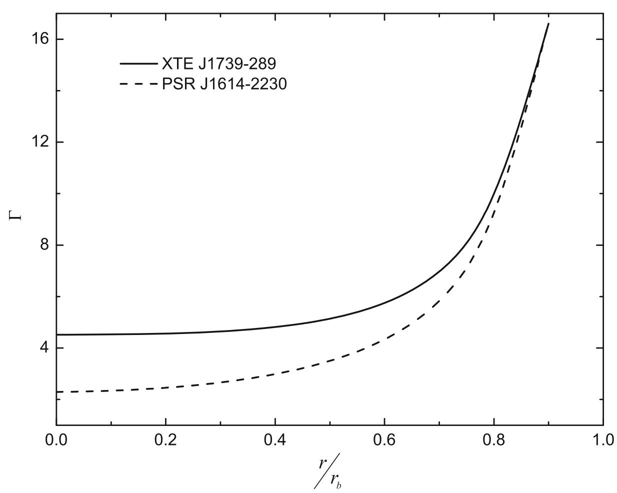

Figure 13. Variation of adiabatic index with radius for XTE J1739-289 and PSR J1614-2230 for the parameters given in table 1.

$$\rho > 0; \quad \rho - p_r \geq 0; \quad \rho - p_t \geq 0; \quad \rho \geq 0;$$
$$\rho - p_r - 2p_t \geq 0; \quad \rho \geq |p_t| \text{ and } |p_r|. \tag{43}$$

7. Results and discussions

It has been observed that the physical parameters ($e^{-\lambda}$, p_r, p_t, ρ, p_r/ρ, p_t/ρ, v_r^2, v_t^2, z) are positive at the centre and monotonically decreasing outward (figures 1–6). However, e^{ν}, anisotropy parameter and adiabatic index are minimum at the centre and increasing outward (figures 1, 6, 7). As seen from figure 8, the stability factor is within $-1 < v_t^2 - v_r^2 < 0$, and therefore the solution is stable. The stable and static stellar configuration can be achieved when all the forces acting on the system via TOV equation are counterbalancing each other (figure 9). The mass–radius relationship and the compactness parameter resulting from the solution are represented in figures 10 and 11 respectively. From figure 12, we can verify our solution satisfying all the energy conditions. The adiabatic index is shown in figure 13 and it is more than $4/3$. All the parameters of the two well-known compact stars XTE J1739-289 and PSR J1614-2230 are presented in table 1 and their masses and radii estimated from our calculations exactly match with the experimentally observed values.

8. Conclusions

We have obtained a new solution of Einstein field equation using Karmarkar condition which is suitable for the realistic modelling of various stars. The solution is well-behaved in all respects and can produce mass and radius comparable to the experimentally observed values. The robustness of our solution is that the calculated values of mass and radius exactly match with the observed values.

The new solution presented here is in fact a special case of a more general solution proposed by Herrera *et al* [19]. They mentioned that all the spherically symmetric solutions can be generated from two primitive generating functions $\zeta(r)$ and $\Pi(r)$ defined as

$$e^{\nu} = \exp\left[\int \left\{2\zeta(r) - \frac{2}{r}\right\} dr\right] \tag{44}$$

$$\Pi(r) = 8\pi(p_r - p_t). \tag{45}$$

These two generating functions corresponding to our solution are given below:

$$\zeta(r) = \frac{5\sqrt{a}bBr(1+br^2)^{3/2}}{5bA + \sqrt{a}B(1+br^2)^{5/2}} + \frac{1}{r} \tag{46}$$

Table 1. Parameters of two well-known compact star candidates XTE J1739-289 and PSR J1614-2230.

Objects	a (km^{-2})	b (km^{-2})	A	B (km^{-1})	R (km)	$M/M_{\odot}$	$2M/R$	z_s	Type
XTE J1739-289	0.004304	0.00092	0.2221	0.0294	10.9	1.51	0.411	0.303	Quark star
PSR J1614-2230	0.003071	0.00030	−0.2112	0.0231	14	1.97	0.417	0.310	Neutron star

$$\Pi(r) = \frac{r^2[3b - a(1+br^2)^4]}{(1+br^2)[1+ar^2(1+br^2)^3]^2[5Ab + B(1+br^2)\sqrt{a(1+br^2)^3}]} \times [a(1+br^2)^3\{5Ab + B(1+br^2)\sqrt{a(1+br^2)^3}\} - 5bB\sqrt{a(1+br^2)^3}]. \tag{47}$$

Acknowledgements

The authors are grateful to the anonymous referee(s) for rigorous review, constructive comments and useful suggestions.

References

[1] A S Eddington, *The mathematical theory of relativity* (Cambridge University Press, Cambridge, 1924)
[2] K R Karmarkar, *Proc. Indian Acad. Sci.* **27**, 56 (1948)
[3] S N Pandey and S P Sharma, *Gen. Relativ. Gravit.* **14**, 113 (1981)
[4] H P Robertson, *Astrophys. J.* **82**, 284 (1933)
[5] K Schwarzschild, *Sitz. Deut. Akad. Wiss. Math. Phys. Berlin* **24**, 424 (1916)
[6] R R Kuzeev, *Gravit. Theor. Otnosit.* **16**, 93 (1980)
[7] J Rayski, *Dublin Institute for Advance Studies* (1976) (Preprint)
[8] M Pavsic and V Tapia, arXiv:gr-qc/0010045 (2001)
[9] M Kohler and K L Chao, *Z. Naturforsch. A* **20**, 1537 (1965)
[10] Y K Gupta and J Kumar, *Astrophys. Space Sci.* **336**, 419 (2011)
[11] S Kumar and Y K Pratibha Gupta, *Int. J. Mod. Phys. A* **25(20)**, 3993 (2010)
[12] T Gangopadhyay *et al, Mon. Not. R. Astron. Soc*. **431**, 3216 (2013)
[13] K N Singh and N Pant, *Astrophys. Space Sci.* **361**, 177 (2016)
[14] K N Singh, N Pant and N Pradhan, *Astrophys. Space Sci.* **361**, 173 (2016)
[15] K N Singh, P Bhar and N Pant, *Int. J. Mod. Phys. D* **25(11)**, 1650099 (2016)
[16] S Thakadiyil and M K Jasim, *Int. J. Theor. Phys.* **52**, 3960 (2013)
[17] L Herrera and N O Santos, *Phys. Rep.* **286**, 53 (1997)
[18] R Chan, L Herrera and N O Santos, *Mon. Not. R. Astron. Soc.* **256**, 533 (1993)
[19] L Herrera, J Ospino and A Di Prisco, *Phys. Rev. D* **77**, 027502 (2008)